J. Fluid Mech. (1982), *vol.* 124, *pp.* 391–409
Printed in Great Britain

On the layers produced by rapidly oscillating a vertical grid in a uniformly stratified fluid

By S. A. THORPE
Institute of Oceanographic Sciences, Wormley, Godalming, Surrey, U.K.

(Received 20 April 1982)

Experiments have been made to examine the fluid motion and density perturbations caused by oscillating a grid of vertical bars horizontally in a uniformly stratified fluid at frequency ω greatly exceeding the buoyancy frequency N. A highly turbulent region is produced near the grid. Beyond this lies a region of intrusive layers as described by Ivey & Corcos (1982), while further from the grid the motion is dominated by internal waves. The boundary between the turbulent region and the intrusive region is clearly defined, and the width of the former region appears to be proportional to $y = a^{\frac{3}{4}}M^{\frac{1}{4}}(\omega/N)^{\frac{1}{2}}$, where a is the amplitude and M the mesh length of the grid. The vertical scale of the layers, which sometimes form to give a regular sequence of high and low density gradients, is also proportional to y. This scaling is shown to be consistent with that found by Hopfinger & Toly (1976) in their study of motion produced by grids oscillating in homogeneous fluids, while the abrupt change in character of the motion at the edge of the turbulent region is in accord with measurements made by Dickey & Mellor (1980) in the wake of a grid drawn steadily through a stratified fluid. The scaling is also in accord with Ivey & Corcos' observations of the width of the turbulent region, the thickness of the layers, and the vertical flux of density.

The observation of the layers is considered in the light of conjectures about the instability of turbulent motion in stratified fluids. The character and conditions of generation of the layers are consistent with their being a manifestation of the instability, but the identification is not conclusive.

1. Introduction

An important aspect of many geophysical phenomena is the interaction between turbulent regions and their surroundings when both are of non-uniform density. Progress in understanding the mechanisms has been aided by laboratory experiments. (For many fine examples see Turner 1973.) In 1976 we made some exploratory experiments in which a grid of horizontal bars was oscillated rapidly up and down a sloping plane boundary in a tank containing a stratified brine solution of constant gradient, the intention being to simulate some of the features of mixing that occurs in the ocean on the continental slopes and around islands. A narrow turbulent region was rapidly established near the grid, while near the bottom of the tank and near the free surface were produced regions of slow circulation. These regions supply and receive a flux of brine carried up the slope both by the turbulence and by a mean flow parallel to the slope. This flow results from the pressure imbalance derived from the turbulently modified density profile, in much the same way as that driven by diffusion at a sloping boundary (Wunsch 1970; Phillips 1970). The effect of grid mixing near the horizontal boundaries at the bottom and top of the slope leads to

the local reduction of the density gradients, and hence to horizontal pressure gradients, which drive the circulations. After becoming established in the first few seconds of grid motion, the turbulent region at the slope appeared to increase its thickness very slowly, if at all. A minute or so later, however, dye dropped into the tank or released from the grid showed the presence of layers beyond the turbulent region spreading horizontally away from the grid.

The cause of these layers was not established. Their spreading was accompanied by patterns of circulation in horizontal planes and their vertical structure was sometimes regular and periodic, of uniform scale. This vertical scale was not much different from the vertical spacing of the oscillating grid bars, which might possibly have acted as local centres of mixing and intrusions. Alternatively it was possible that the layers could have grown in succession from the top and bottom of the slope in the manner described in another context by Mendenhall & Mason (1923) (for further discussion see Thorpe, Hutt & Soulsby 1969).

Our interest was rekindled by a recent paper by Ivey & Corcos (1982), who described experiments in which a plate with horizontal square grooves forming a grid was oscillated vertically at the end of a long tank filled with a uniform gradient of brine. A region of highly turbulent motion was generated near the grid, and its width was measured, as well as the vertical flux of density. Ivey & Corcos used a conductivity probe to measure vertical profiles of density in the tank, and observed spreading layers formed beyond the turbulent region some minutes after the commencement of grid motion. These were sometimes very regular in height and of scale similar to that of the grid but, by making experiments over a range of grid frequencies ω, amplitudes a and buoyancy frequencies N, it was demonstrated that the scale of these intrusions showed some variation. (Ivey & Corcos chose to plot the height of the layers versus $a\omega/N$, and obtained a scatter of points that suggested a linear relationship, though not one passing through the origin.)

The observed regular and vertically periodic nature of the layers reported by Ivey & Corcos, and observed in the sloping-grid experiments, suggested that their generation might be due to more subtle effects than, for example, simply the occasional collapse of randomly occurring large blobs of mixed fluid generated in the turbulent region near the grid. Their study is of interest in connection with conjectures that have been made regarding the possible instability of turbulent stratified flow (see §4) and it seemed worthwhile making some experiments in which the possibility of layer formation at, or near, the vertical scale imposed by the presence of the horizontal bars could be avoided. In the course of these experiments, described in §2, some scaling relationships became apparent that suggested a connection between features observed in these experiments and those in which a grid is drawn steadily through a stratified fluid.

2. Experiments

Preliminary experiments were made in which a grid of vertical bars was oscillated horizontally in its own plane, parallel to and near one of the endwalls of a rectangular Perspex tank. The bars were made of Perspex and were connected by horizontal bars at top and bottom. Turbulence was generated in the stratified brine solution near the grid, but after a minute or so almost circular horizontal circulations were set up in the centre of the tank that tended to advect turbulence away from the neighbourhood of the grid. We suspected that the circulation and turbulence might be affected by slight distortions in the grid bars, and so two narrow horizontal tie

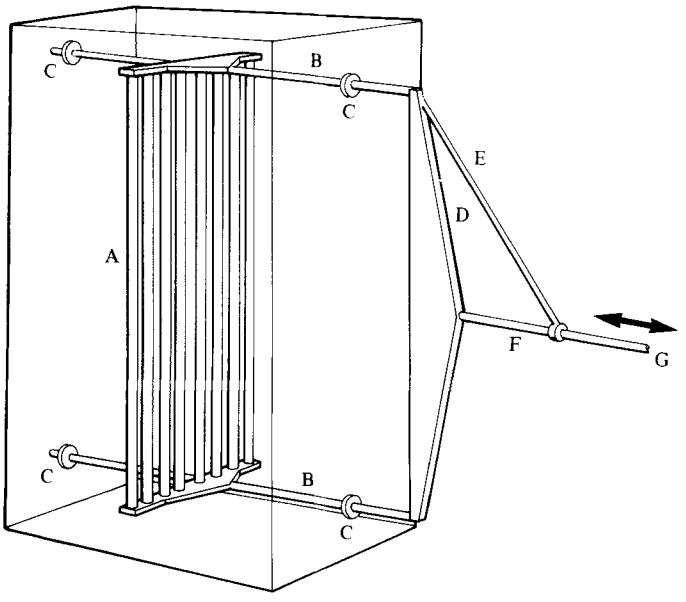

FIGURE 1. The apparatus. The Perspex tank of height 30·5 cm, width 20·3 cm and breadth 15·2 cm contains a grid A of eight vertical bars of square cross-section, supported by pistons B, which pass through watertight seals C. The pistons are driven via linkage bars D, E, F and eccentric cam by a variable-speed motor. Inlet and outlet tubes are provided in the bottom and top of the tank.

bars were added passing through the grid some way from their ends. The effect was profound, resulting in the rapid generation of two very distinct layers of large vertical density gradient at the level of the tie bars shortly after the grid oscillation was started, although there was little change in the circulation. An explanation for the layers is that the tie rods locally reduced the vortex shedding from the grid and hence the local diffusivity and vertical flux. At other levels the flux is maintained, however, resulting in an increase in density below the level of the tie rods and a decrease above, and hence to the generation of the two density interfaces. The observations counsel caution in making and interpreting experiments in which the stirring is not uniform with height.

In view of the undesirable effects of the circulation, a new tank was constructed (figure 1) in which the vertical grid was oscillated in a direction normal to its own plane, and this fortunately did not produce the unwanted strong circulations. The tank dimensions (see the caption to figure 1) were limited, and the size was perhaps somewhat less than ideal. The grid was constructed of square bars of side 0·64 cm with 1·91 cm between centres (the 'mesh length' M). Experiments were made with the grid positioned either in mid-tank or close to one wall. The grid amplitude a was varied between 0·28 and 0·94 cm and the frequency ω between 12·3 and 37·0 rad s^{-1}. The buoyancy frequency N in the tank was closely uniform and was varied between 0·56 and 2·52 rad s^{-1}. Flow visualization was achieved by conventional shadowgraph streak photogaphy (using aluminium particles) and dye, and still and ciné cameras were used. Figure 2 is a sketch of the main features seen in the experiments and the notation used to denote the scales that we discuss below.

Figure 3 shows a typical experiment in which columns of dye have been produced by slowly lowering and raising a fine rod with potassium permanganate crystals stuck onto the lower end before starting the grid (figure 3*a*). On the commencement of

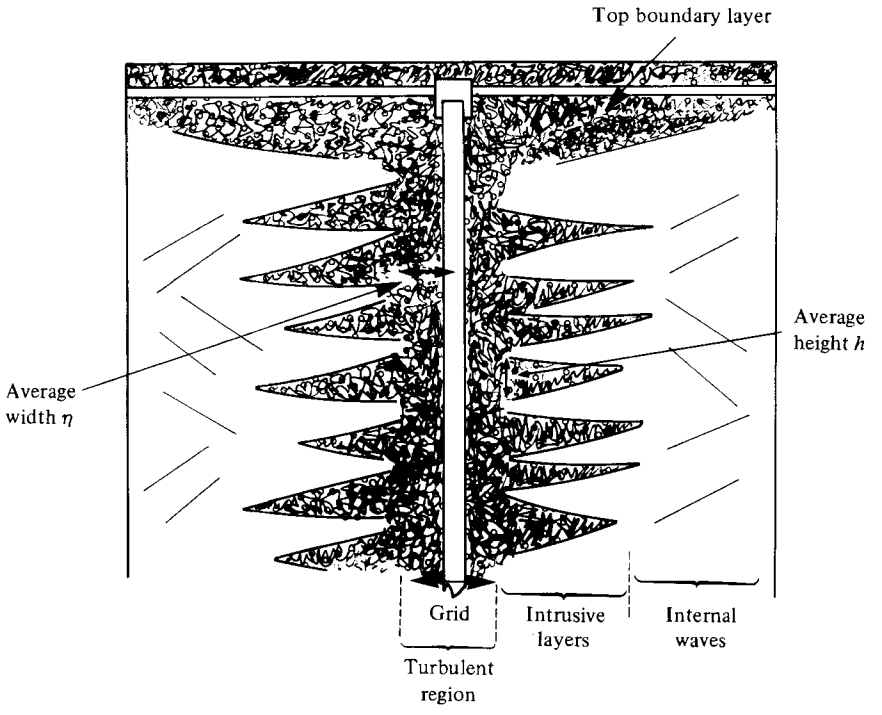

FIGURE 2. Sketch showing the main features seen in the experiment. Only the top half of the tank is shown.

motion dye near the grid at the centre of the tank is rapidly spread sideways with vertically regular, small-scale protuberances shed from the grid being visible during the first second or two of its motion (see also figure 8*a* below) and the column of dye being split into two or more columns (figure 3*b*). The periodic vertical structure has an average scale (measured over 14 experiments) of $0{\cdot}42 \pm 0{\cdot}10$ cm and may be due to Rayleigh–Taylor vortices occurring in the eddies with vertical axes shed by the grid bars as they accelerate. The columns rapidly coalesce (figure 3*c*), with the leading edges having now larger rounded protuberances, which spread horizontally and collapse, sometimes with evidence of a structure resembling a vortex ring at the leading edge (see e.g. figures 2(*d*, *e*), at right, about a third of the way up). Such rings occasionally become detached from the main dye cloud. Deeper layers are formed at the top and bottom of the tank, being mixed partly by the horizontal bars supporting the grid. These top and bottom boundary layers receive and supply the vertical flux of brine in the turbulent motion generated by the grid. Our objective here, however, is to describe the character of the region well away from these layers at times when their thickness is much less than the tank height and their immediate influence on the flow or properties of the fluid in the interior of the tank is negligible. Measurements were therefore made over a vertical extent that excludes these top and bottom layers.

Dye seen at the left of figure 3 outside the spreading coloured region is distorted by the collapsing protuberances or intrusions, dye between them being carried towards the grid and rapidly mixed by small-scale turbulence. The interfaces marked by nearly horizontal lines of dye (see figure 3*f*) resulting from this distortion are seen to be disturbed by small-scale waves propagating from the grid. Dye near the

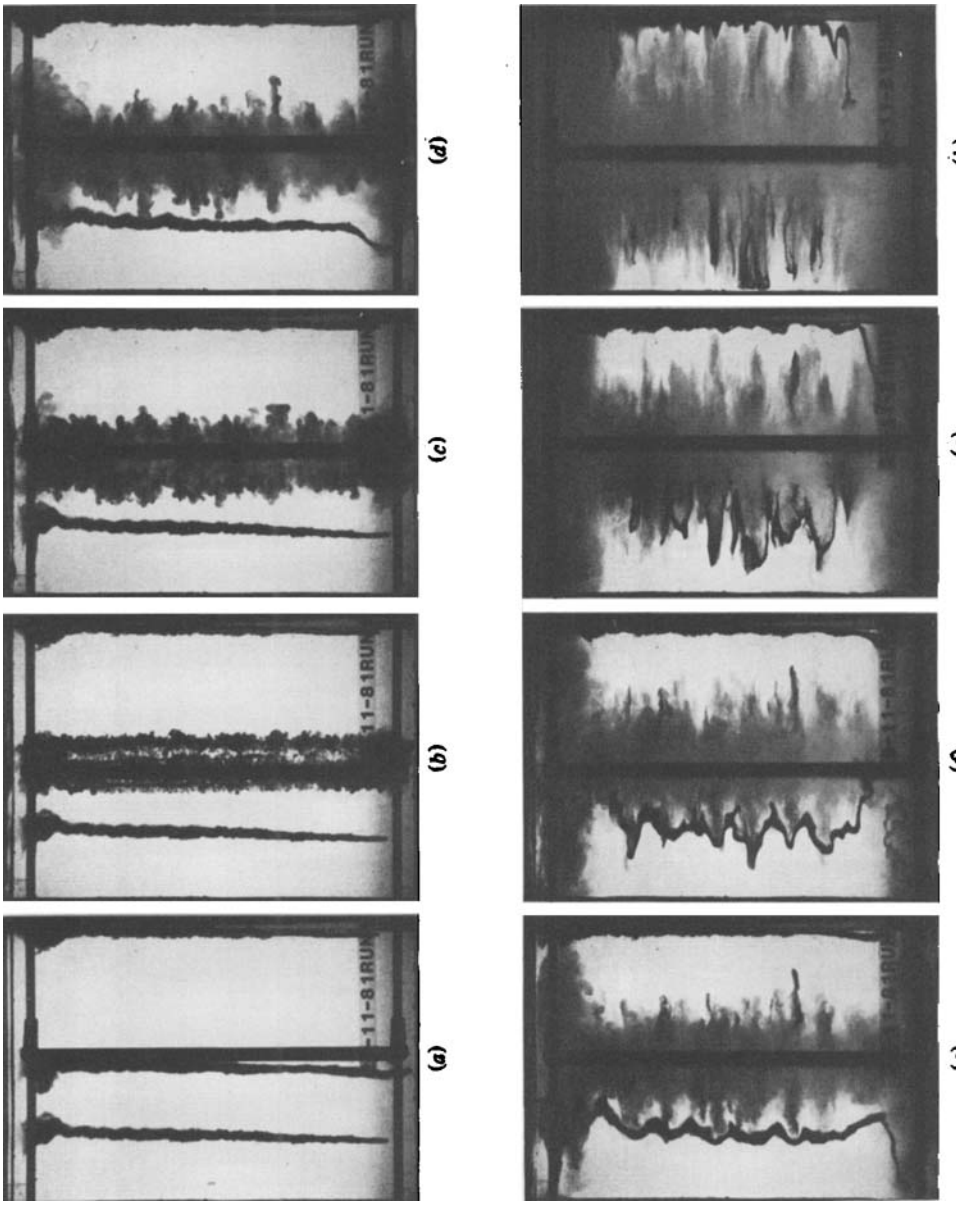

FIGURE 3. Experiment with three columns of dye added to the brine solution. The grid is seen end-on in mid-tank, and the tank width is 20·3 cm; $a = 0{\cdot}94$ cm, $\omega = 21{\cdot}3$ rad s^{-1}, $N = 1{\cdot}98$ rad s^{-1}. Photos at times after start (*a*) 0; (*b*) 0·5 s; (*c*) 1·4 s; (*d*) 3·2 s; (*e*) 5·4 s; (*f*) 11·1 s; (*g*) 20·1 s; (*h*) 57·3 s.

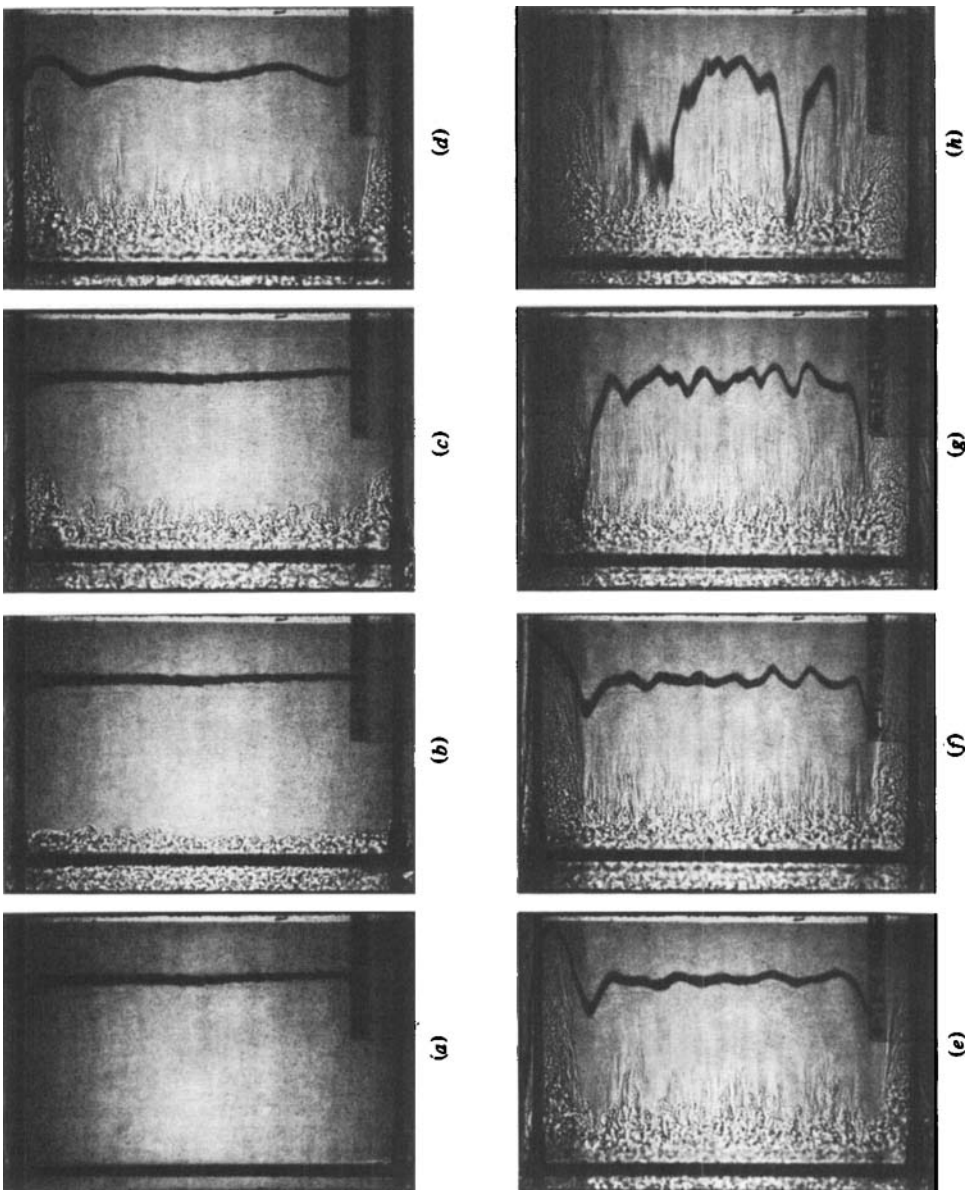

FIGURE 4. Shadowgraph with grid oscillating near the left-hand wall. Tank width is 20·3 cm; $a = 0.59$ cm, $\omega = 24.7$ rad s^{-1}, $N = 1.98$ rad s^{-1}. Photos at times: (*a*) 0·5 s; (*b*) 0·9 s; (*c*) 4·4 s; (*d*) 9·7 s; (*e*) 18·7 s; (*f*) 29·3 s; (*g*) 69·7 s; (*h*) 239·2 s.

right-hand sidewall spreads predominantly sideways along the wall in a sinusoidal pattern on the scale of the intrusions and is only slowly diffused away from the wall.

Shadowgraph pictures (figure 4) indicate a similar development, but show more clearly the presence of the three regions at mid-depth in the tank sketched in figure 2. The first, surrounding the grid, is turbulent and is dominated by small-scale incoherent motions. It becomes established within a few seconds of the commencement of grid motion and thereafter retains an almost constant width. Beyond this is a region of multiple intrusive flows, and yet further from the grid is a region in which signs of overturn are rare and motion is dominated by internal waves. These waves can be seen in the original shadowgraph films as dark shadows propagating at large angles to the horizontal. The edge of the turbulent region is quite distinct in the ciné film, being marked by an abrupt change in the structure of the flow.

The development of disturbances seen in the dye line at the right of figure 4 can be ascribed to the arrival of internal waves of increasing vertical wavenumber produced at the grid. The horizontal group velocity of internal waves is

$$c_{gx} = \frac{N^2 m^2 k}{(k^2+l^2)^{\frac{1}{2}}(k^2+l^2+m^2)^{\frac{3}{2}}}, \tag{1}$$

where k, l, m are the wavenumbers in the horizontal directions away from the grid and across the grid, and in the vertical direction respectively. For fixed m, c_{gx} is maximum when $k = l = 0$;

$$\max c_{gx} = \frac{N}{m}. \tag{2}$$

At a fixed distance s the vertical wavenumber of the waves arriving from a source of white noise is given by $s/t = \max c_{gx}$, and thus m increases as time t increases. This relationship is roughly supported by the observations, both in the time of the arrival of disturbances† and in the reduction of the vertical scale of the dye disturbance seen, for example, between figures 4(*e*) and (*f*). The scale of the disturbance of the dye column decreases to a scale similar to that of the advancing intrusions and becomes a permanent distortion. In figure 4(*h*) the upper part of the dye column has been carried around the back of the tank by a slow circulation induced by the collapse of fluid in the intrusive region. Fine horizontal layers can be seen beyond the region of active intrusions. These are similar in appearance to the structures seen in the collapsed wake of a grid or body drawn horizontally through a stratified fluid.

Two stages in the development of the motion are shown by the streak photographs (figure 5*a*, *b*). The spreading intrusive flows are seen soon after the commencement of grid motion in figure 5(*a*) as groups of short, almost horizontal, lines on each side of the grid about a quarter of the distance from the grid to the sidewalls. Between these the streaks indicate a divergent flow as fluid is forced to move vertically away from the advancing intrusions. Figure 5(*b*) shows the more-energetic field of motion about five minutes after the grid motion commenced. The camera exposure time was about 1·1 times the buoyancy period N, and the streaks show a superposition of advection and oscillatory flow with period somewhat greater than the buoyancy period. The internal waves were particularly noticeable in their production of vertical motions near the sidewalls (especially in the experiments using dye) but, as figure 5(*b*) shows, have an effect quite near the grid. This photograph is at a time when the waves of 1 cm vertical wavelength generated by the grid would have travelled four

† For example in figure 4(*e*) the vertical wavelength in the dye column is about 2·9 cm, and hence (2) gives $\max c_{gx} = 0{\cdot}91$ cm s^{-1} compared with $s/t = 0{\cdot}78$ cm s^{-1}.

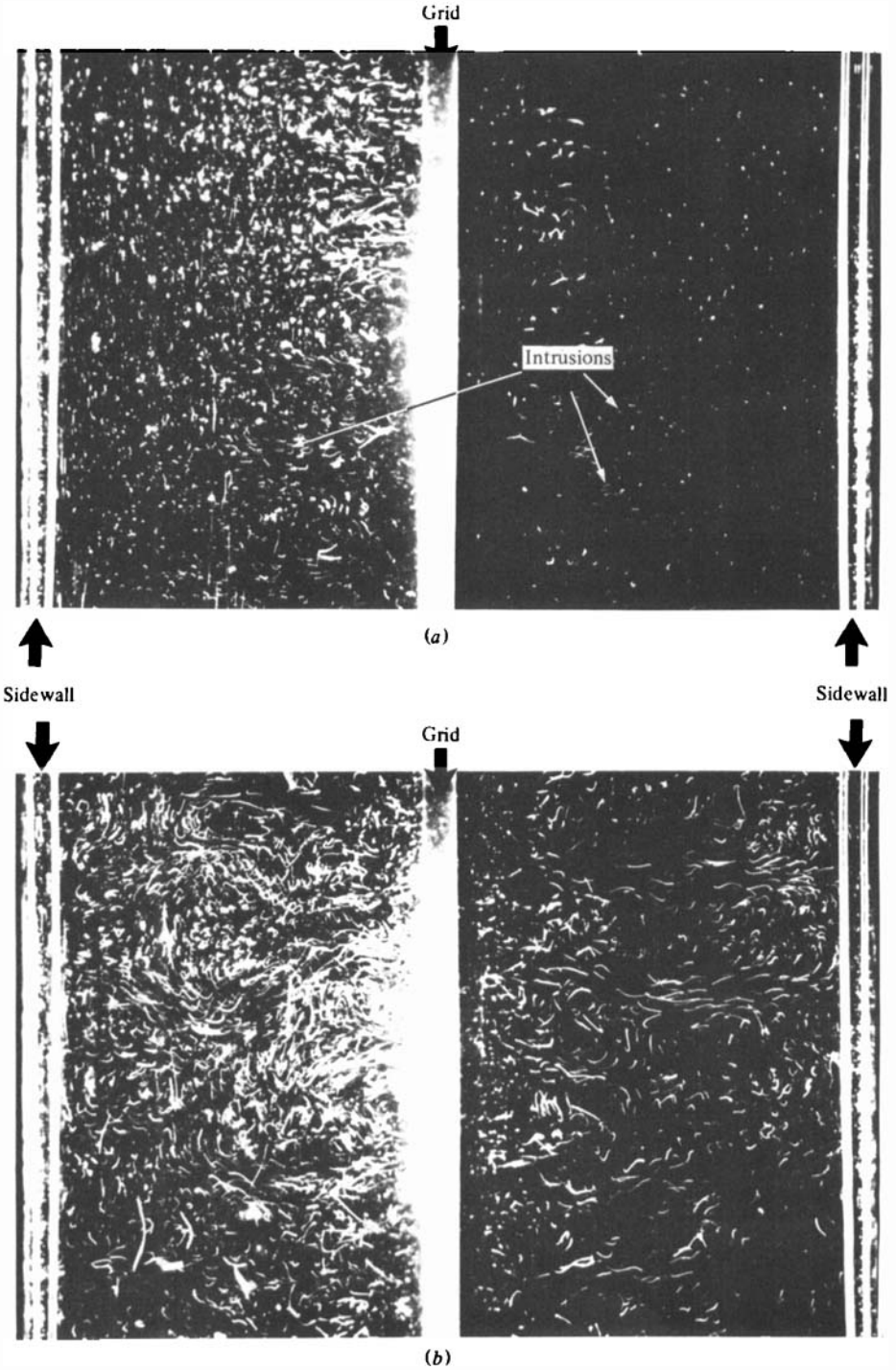

FIGURE 5. For caption see facing page.

times the tank width (using (2)) and hence the near-grid intrusive flow is affected by waves reflected from the sidewalls.

The mean width η of the turbulent near-grid layer, measured from the mid-point of grid motion (see figure 2), was measured from the ciné films about 20–100 s after the commencement of the grid motion, selecting part of the tank well away from the circulating layers at the top and bottom. The mean height h of the intrusions was similarly measured from the shadowgraph photographs by measuring the average height of the regions of small-scale structures composing the intrusions at a position close to the edge of the turbulent region. This was not a very precise measurement, but provided a measure which corresponded reasonably well to a scale estimated by Ivey & Corcos (1982). They measured the vertical distance between the intersections of tangents drawn through the inflexion points in the vertical profiles of density (at the edge of the layers) and lines of constant density drawn in the centre of the layers, and thus approximately the height of the region of uniform density in the layers. This scale was less than the average distance between the centres of density interfaces, the scale ratio† being about $1{\cdot}45 \pm 0{\cdot}13$.

Figure 6 shows how η and h vary with the lengthscale

$$y = a^{\frac{3}{4}} M^{\frac{1}{4}} \left(\frac{\omega}{N}\right)^{\frac{1}{2}}. \tag{3}$$

The choice of y will be explained in §3. The trend in each set of points is approximately linear, with

$$\eta = 0{\cdot}94y, \quad h = 0{\cdot}34y, \tag{4), (5}$$

being the best-fitted lines through the origins.

The mean width l_d of the central dyed regions (as seen in figure 3), the mean width l_s of the region of small-scale structures (shown by the shadowgraphs), and the length l_i of individual spreading intrusions were also measured from the photographs as functions of time. (Both l_d and l_s may be criticized as adequate descriptions of the dispersive process since the photographs show the furthest penetrating intrusion at any level and not by the average.) Since y provides a scale for the height of the intrusions (equation (5)) it was natural to normalize l_d, l_s and l_i with y and to plot against the non-dimensional time Nt. As an example, the plots of l_s versus y are shown in figure 7. Data collapsed reasonably well onto

$$\frac{l_d}{y} = 0{\cdot}50(Nt)^{0{\cdot}38} \quad (2 \leqslant Nt \leqslant 20), \tag{6}$$

$$\frac{l_s}{y} = 0{\cdot}55(Nt)^{0{\cdot}40} \quad (2 \leqslant Nt \leqslant 25), \tag{7}$$

$$\frac{l_i}{y} = 0{\cdot}53(Nt)^{0{\cdot}44} \quad (2 \leqslant Nt \leqslant 20). \tag{8}$$

† This was estimated by measuring profiles presented by Ivey and Corcos and from information provided (G. N. Ivey, private communication).

FIGURE 5. Streaklines produced by particles of aluminium suspended in the brine solution. The particles are illuminated by a collimated beam of light passing through a vertical slot 1·9 cm wide in the centre of the left-hand wall. The beam width was reduced in passing through the grid, seen indistinctly at the centre, which accounts for the difference in appearance of the left and right halves of the tank. The distance between the vertical rods at the two sides of the tank (introduced to give a scale) is 19·6 cm, and $a = 0{\cdot}4$ cm, $\omega = 29{\cdot}2$ rad s^{-1}, $N = 1{\cdot}73$ rad s^{-1}. The exposure time was 4 s. Photos at mean times after starting the grid: (*a*) 3 s; (*b*) 302 s. The vertical lines seen at the left are due to slowly rising gas bubbles. Near the grid the motions are three-dimensional and the streaks do not give an adequate impression of the motion.

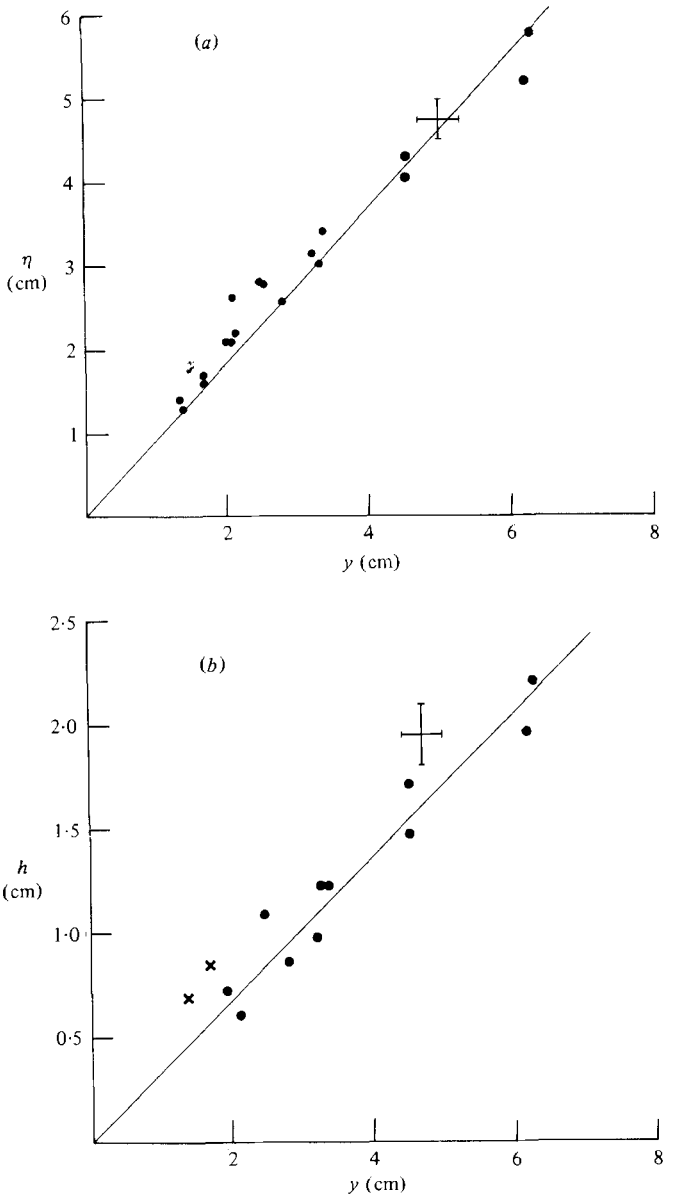

FIGURE 6. (*a*) The variation of the width η of the turbulent region with $y = a^{\frac{3}{4}}M^{\frac{1}{4}}(\omega/N)^{\frac{1}{2}}$. (*b*) The variation of the mean height h of the intrusive layers measured at the edge of the turbulent region with y. The points × show the average height of layers in the narrowed tank (see figure 8 and §4).

The difference between l_d and l_s appears to be insignificant. Earlier laboratory observations of collapsing regions (see e.g. Wu 1969; Amen & Maxworthy 1980) are of single intrusions, and cannot be directly compared with these measurements of *multiple* intrusions, although it is interesting to notice the reported presence of strong internal waves in all cases studied.

Although the range of the vertical scales of the intrusions in any one experiment appeared to be small, in general no very regular pattern was visible and the resulting layers appeared to be transient in position. When the grid motion was arrested after

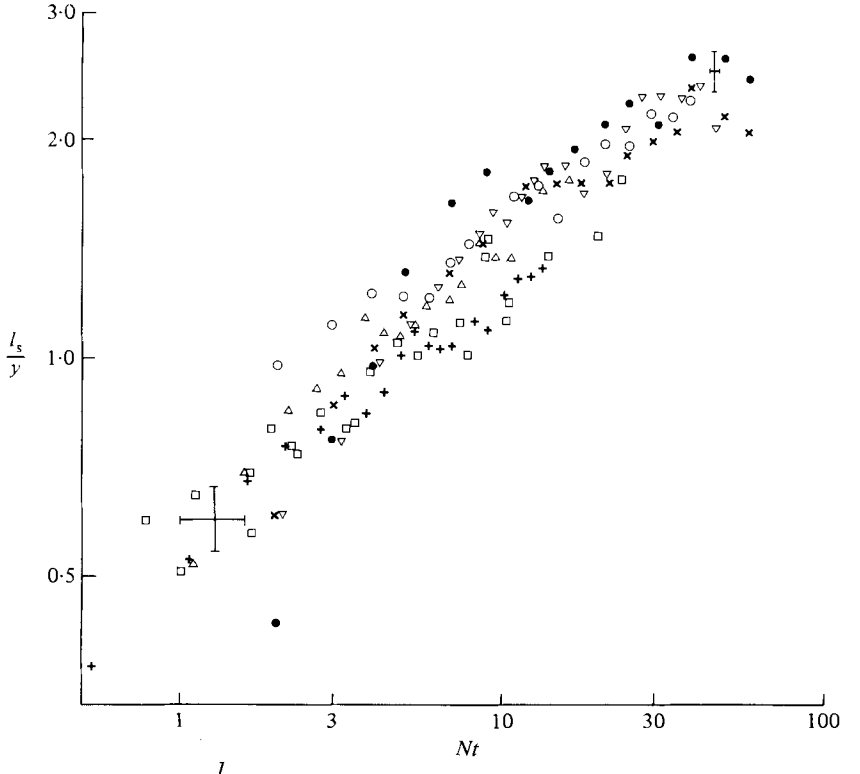

FIGURE 7. The variation of $\frac{l_s}{y}$ with Nt, plotted on logarithmic scales, for the following sets of values of a (cm), ω (rad s^{-1}) and N (rad s^{-1}): ●, 0·59, 12·3, 2·00; ×, 0·59, 24·7, 1·98; ⊙, 0·59, 34·9, 2·01; △, 0·59, 35·0, 1·08; □, 0·59, 35·0, 0·56; +, 0·93, 34·3, 1·09; ▽, 0·33, 36·6, 2·12.

some 5 min stirring, no uniform array of shadows produced by layers could be detected, as might have been expected from Ivey & Corcos' experiments. Stopping the grid resulted in a rapid decay of the turbulent motion and left a field of small-scale horizontal striations like those remarked on in figure 4, as well as internal waves which continued for a minute or two. It seems likely that the internal waves confined and reflected from the walls in the present experiment (but able to radiate and dissipate in the larger tank in Ivey & Corcos' apparatus) may have disrupted the regularity of the layer spacing.

A further important observation was made when the grid motion was stopped. There was no tendency for motions to occur, which would suggest that the mean vertical gradient near the grid was different from that in the intrusive region or in the internal wave region. It thus appears that, although violently stirred by the grid, the mean density gradient in the turbulent region remains equal to that outside the turbulent region, except in the circulatory regions at the top and bottom of the grid. This is not the case in experiments when a grid is inclined to the vertical (see §1), or when it is horizontal, or, with a vertical stirrer, when the mixing is inhomogeneous in the vertical. Then the mean vertical density profile, and hence N, is modified by the mixing produced by the grid. During the short period before the estimates of η and h were obtained the absence of vertical motion of the dye indicates that the density in the central part of the tank did not change, and hence that the buoyancy frequency in the turbulent region remained at its original measured value N.

For comparison with the stratified system, we measured the time before turbulence arrived at a rod covered with dye crystals at a distance of 5·1 cm from the grid after the grid motion was started from rest in fresh water (i.e. no stratification). Judgment of the time was somewhat subjective, but approximately

$$t\ (\mathrm{s}) = 2{\cdot}33 \times 10^{4}\omega^{-2{\cdot}4}, \tag{9}$$

for $a = 0{\cdot}94$ cm, 16 rad s^{-1} $< \omega <$ 32 rad s^{-1}.

3. Analysis

We shall suppose that the scaling of all the motions in the tank is determined by the properties of the turbulent region, and that these can be described by dynamics and associated scales formed by Hopfinger & Toly (1976) in their study of motion induced by a square grid of square bars. It is implicit in this assumption that sufficiently close to the grid the motion is unaffected by the stratification. Then retaining Hopfinger & Toly's notation for constants C and β, the root-mean-square velocity u at a distance x from the mean grid position is given approximately by

$$u = \frac{\sqrt{2}\, C\omega a^{\frac{3}{2}} M^{\frac{1}{2}}}{\pi} \frac{}{x}, \tag{10}$$

and the integral lengthscale l of the motion is

$$l = \beta x. \tag{11}$$

The eddy timescale $l/u = \beta\pi x^2/\sqrt{2}\, C\omega a^{\frac{3}{2}} M^{\frac{1}{2}}$ increases with distance from the grid. At some distance x_c the eddies will suffer significant collapse, under the effects of stratification, in a time that is less than l/u. Beyond this distance from the grid the turbulent will change in character, and the scaling laws (10) and (11) will no longer be valid. Since, as we remarked in §2, N is uniform, we might suppose the distance is given by some critical value of the local parameter u/lN, that is

$$\frac{u}{lN} = \gamma, \tag{12}$$

where γ is a constant. This leads to

$$x_c = \frac{2^{\frac{1}{4}} C^{\frac{1}{2}} a^{\frac{3}{4}} M^{\frac{1}{4}}}{\beta^{\frac{1}{2}} \pi^{\frac{1}{2}} \gamma^{\frac{1}{2}}} \left(\frac{w}{N}\right)^{\frac{1}{2}} \tag{13}$$

$$= \frac{2^{\frac{1}{4}} C^{\frac{1}{2}}}{\beta^{\frac{1}{2}} \pi^{\frac{1}{2}} \gamma^{\frac{1}{2}}} y, \tag{14}$$

using the lengthscale y defined in (3). The distance x_c is then directly proportional to y.

Evidence that a condition of the type expressed by (12) holds is to be found in the experiments of Dickey & Mellor (1980). In those experiments a horizontal grid of square bars was raised vertically through a stratified fluid. An abrupt change in character of the motion from turbulence to internal waves occurred some distance behind the grid where approximately

$$\frac{u}{lN} = 0{\cdot}27 \tag{15}$$

(Dickey & Mellor's equation (23)), and here the rate of decay of turbulent kinetic energy departed sharply from that found in neutral stratification. The parameter γ^{-2} is a measure of the local Richardson number. Near the grid, where this is less than about 14, the motion is hardly affected by stratification. At greater distances stratification becomes important.

The integral lengthscale at distance x_c from the grid is

$$l_c = \beta x_c \tag{16}$$

$$= \frac{2^{\frac{1}{4}} C^{\frac{1}{2}} \beta^{\frac{1}{2}}}{\pi^{\frac{1}{2}} \gamma^{\frac{1}{2}}} y. \tag{17}$$

It is plausible that the integral lengthscale l_c of the turbulent motion near its point of collapse provides a vertical scale h for the intrusive layers determined experimentally in (5). Tentatively equating h with l_c (in 17), and the estimate of the width x_c of the turbulent region (in 14) with that observed η (in 4), we find

$$\beta = 0{\cdot}36, \quad C = 0{\cdot}70\gamma. \tag{18), (19}$$

If further we identify γ (in 12) with the constant found by Dickey & Mellor (in 15), then

$$C = 0{\cdot}19. \tag{20}$$

Values of C and β will depend upon the geometry of the grid used, and (if we accept the identification of h with l_c) it is thus not surprising that C (in 20) is less than the value found by Hopfinger & Toly, approximately 0·25. They observed a variety of values of β between 0·1 and 0·35, depending (in no direct way) on a and M. If Hopfinger & Toly's scaling is appropriate (and the relationships (6)–(8) support the hypothesis) the experimental results of figure 6 suggest that β is probably not a strong function of a in the range covered.

We now adopt the scaling laws (10) and (11) and see if they are consistent with the experimental results of Ivey & Corcos. Ivey has kindly provided the observed values of a, ω, N and η, as well as the estimates of the vertical scale h of the intrusions defined by the intersections of local tangents to the density-versus-depth curve as explained in §2. Omitting one estimate in which the accuracy of the measured η was doubtful, we find a best linear fit to the remaining ten estimates:

$$\eta = 1{\cdot}31y, \tag{21}$$

where we have used $M = 2{\cdot}54$ cm appropriate to these experiments. The mean value of η is 11·9 cm, with a root-mean-square error in the estimate (21) of 2·7 cm. The fit is not perfect but it was difficult to assess η very accurately. Twenty-seven estimates of h were made. With the exception of one set of three points for which $a\omega/N$ is large and h was becoming difficult to determine accurately, Ivey & Corcos' values lie close to

$$h = 0{\cdot}32y, \tag{22}$$

with a mean value of h of 1·88 cm and a root-mean-square error in the estimate (22) of 0·21 cm. Using again the value $\gamma = 0{\cdot}27$ obtained from Dickey & Mellor's experiments, and identifying h with l_c, we find

$$\beta_I = 0{\cdot}24, \quad C_I = 0{\cdot}25, \tag{23), (24}$$

where the subscripts indicate that the constants are those of Ivey & Corcos' grid. These values are again consistent with those found by Hopfinger & Toly. They differ

from these found in (18) and (20); not surprisingly, for the two grids were very different, Ivey & Corcos' grid being of horizontal grooves cut into a plate oscillating vertically in its own plane and the present grid being of vertical bars oscillating horizontally at right angles to the grid plane.

We may extend the comparison to consider the net vertical flux F of density per unit of the tank. From their experiments Ivey & Corcos found that

$$F \propto \omega^{1\cdot6} a^{2\cdot7} N^{1\cdot52} \tag{25}$$

(where the exponents were determined by best fits to the data), and that very little vertical mass flux occurs in the interior of the fluid as a result of the intrusions, the great majority occurring within the turbulent near-grid region. (It is interesting to note, however, that the intrusions are very active in transporting neutral tracers, for example the dye in figure 3, horizontally into the interior.) If the turbulent region behaves much as a region of neutral stability, as suggested by Dickey & Mellor's work, we may assume that the effective eddy-diffusion coefficient K is given by

$$K = qul, \tag{26}$$

where u and l are given by (10) and (11) respectively, and q is a constant. Then K is independent of x, and the vertical flux in the turbulent region will be

$$F = -K\frac{d\rho_0}{dz}, \tag{27}$$

where $d\rho_0/dz = -\rho_0 N^2/g$ is the density gradient, the same in the turbulent region as in the surrounding fluid, and ρ_0 is a reference density. Substituting from (21) and (13), with $\eta = x_c$ we find

$$F = \frac{\rho_0}{g}\left[\frac{C_I^{\frac{3}{2}} q\, 2^{\frac{3}{4}}}{\pi^{\frac{3}{4}}\gamma^{\frac{1}{2}}}\beta_I^{\frac{1}{2}}\right] a^{\frac{9}{4}} M^{\frac{3}{4}} \omega^{\frac{3}{2}} N^{\frac{3}{2}}. \tag{28}$$

Comparing this with the experimental result (25), assuming that the flux is totally transported in the turbulent region, we find the exponents of ω and N to be in excellent agreement; that of a is less satisfactory but not an unreasonable fit. Ivey & Corcos fitted their data to the dimensionally correct curve

$$F = \frac{\rho_0}{g} B a^3 \omega^{\frac{3}{2}} N^{\frac{3}{2}}, \tag{29}$$

and found the constant B was approximately 0·05. Taking appropriate mean values and the form (28), together with values of C_I and β_I given by (24), (23) and $M = 2{\cdot}54$ cm for their grid, we find approximately

$$q = 0{\cdot}20. \tag{30}$$

Using (26) and $a = 0{\cdot}6$ cm, $\omega = 30$ rad s^{-1}, a typical value of K in Ivey & Corcos' experiments would then be 0·12 cm^2 s^{-1}, which, as expected, is much greater than the molecular value. An attempt was made to assess the estimate (30) and variation of K (26) with a and ω ($K \propto a^{\frac{3}{2}}\omega$, using (10) and (11)) by examining the dispersal of dye from a fixed point on a rod introduced quickly into the tank near the grid in the present experiments when the tank was filled with fresh water and after the grid had been oscillating for some time. Diffusion was estimated by assessing the area of dye by eye a few seconds after release. Although roughly in accord with (26) and producing diffusion on scales consistent with (30) no adequate quantitative estimates or comparisons were possible. It is interesting to note that (26) gives an estimate of

diffusion over a distance s, in time t, $s \propto K^{\frac{1}{2}}t^{\frac{1}{2}} \propto \omega^{\frac{1}{2}}t^{\frac{1}{2}}$ (using (26) and (10)), so that, at constant s, $t \propto \omega^{-1}$, in contrast with the front of a spreading turbulent region where $t \propto \omega^{-2\cdot4}$ (determined experimentally, (9)). In the former, dye is spread by motions totally within the turbulent region; in the latter, spread is produced by the entrainment of laminar fluid into the turbulent region. The processes are quite distinct.

4. Discussion

The results are consistent with the scaling laws for fluid motion near grids found by Hopfinger & Toly (1976) and, like the observations of Dickey & Mellor (1980), suggest an abrupt change in the character of turbulence when the intrinsic timescale becomes comparable to the buoyancy period. Intrusive layers were observed beyond the turbulent region. Their scale is consistent with that of the turbulence, but the occurrence of the vertically periodic and regular series of layers reported by Ivey & Corcos has not yet been explained.

Recalling that the mean gradient in the turbulent region is the same as that outside, we may write a Richardson number to characterize the turbulent motion near the grid in the form N^2l^2/u^2. This increases as x^4. Far from the grid the motions decay and hence it may be expected that the Richardson number R of the local motion increases with x and becomes indefinitely large. Linden (1979) has reviewed results of several laboratory experiments in connection with arguments advanced by Phillips (1972) and Posmentier (1977) that turbulence in a stratified fluid may, in some cases, be unstable, in the sense that it will lead to a transition from a uniform density gradient to another density structure. He showed that a necessary condition for the instability discussed by Posmentier, namely that the density flux decreases with increasing density gradient, was equivalent to a condition that the flux Richardson number R_f decreases with increasing R. Such a relationship is apparently satisfied at sufficiently large R in a number of experiments, including those in which motion is induced by moving grids. The instability should produce the evolution of a vertically periodic succession of layers of large and small density gradients. Its rate of growth increases indefinitely as the vertical scale of the layers decreases; however, for the analysis to be valid, it is assumed that the scales of the turbulence must be small compared with the scale of the instability. An ill-defined lower bound is thus imposed on the unstable wavelengths; the vertical scale of most rapidly growing layers has not been predicted.

Although Kranenburg (1982) has criticised the basis of the speculations, arguing that the flux equation using eddy-diffusion coefficients is inappropriate when describing the stability of the turbulent flow, it is nevertheless intriguing to see whether the present experiments support the concept of instability. May the layers be a result not simply of the collapse of turbulent eddies in stratified surroundings, but of local instability of the turbulence?

In our experiments turbulence is locally maintained (unlike Dickey & Mellor's experiment) although it decays with distance from the grid and, if the motion is unstable locally, the instability may have time to develop before the turbulence itself decays. Whether or not instability can develop (supposing that the motion is indeed unstable in some region) will depend on the rate at which energy may be lost by radiation from the potentially unstable motions. If the loss of energy by radiating internal waves and horizontal spread of a locally unstable structure is inhibited, the instability should grow more rapidly. To investigate this idea, we made an experiment

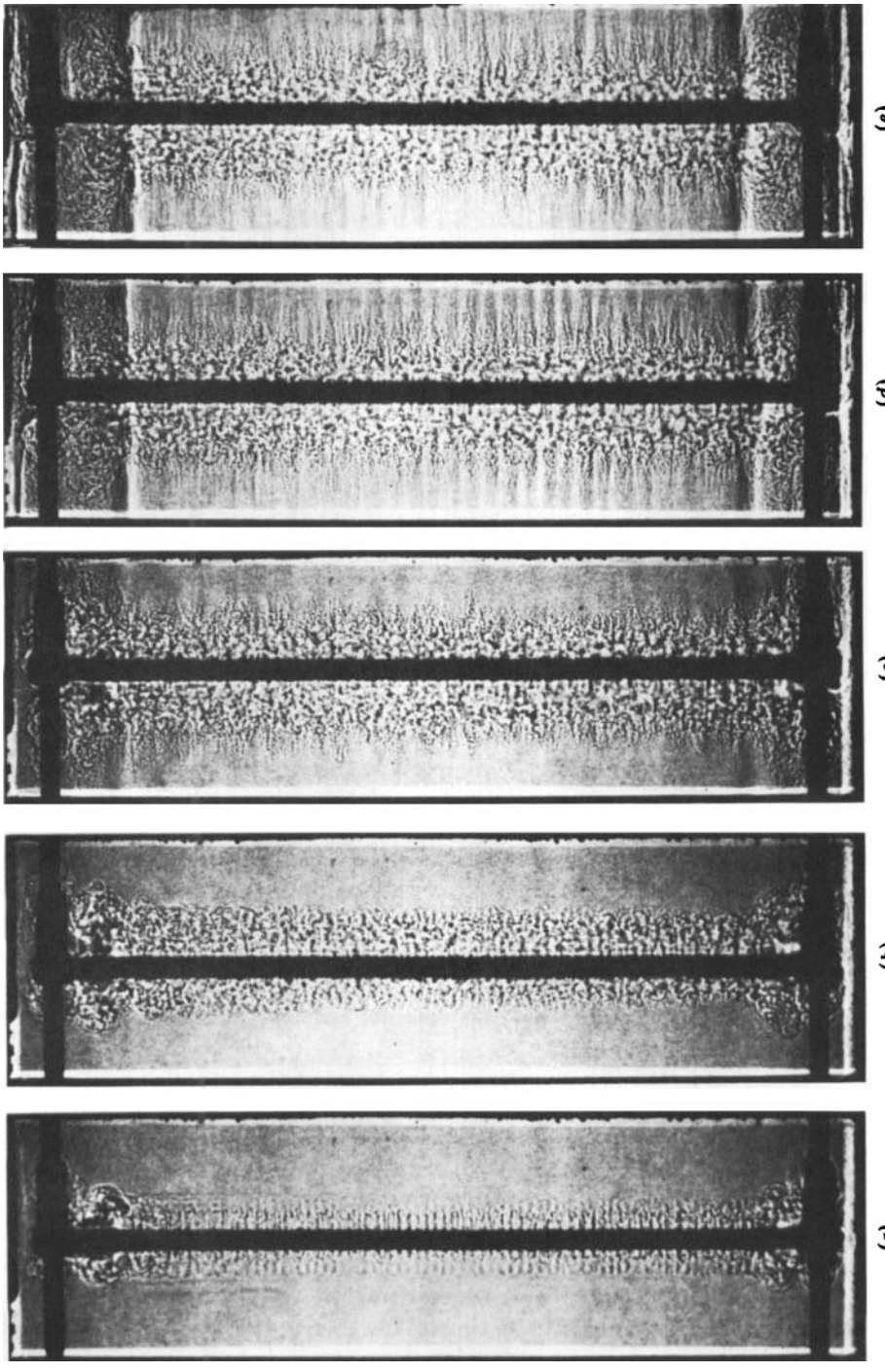

FIGURE 8. Shadowgraph experiment in a compartment 8·5 cm wide with the grid oscillating in the centre; $a = 0{\cdot}31$ cm, $\omega = 15{\cdot}1$ rad s^{-1}, $N = 1{\cdot}94$ rad s^{-1}. Photos at times: (*a*) 1·8 s; (*b*) 3·2 s; (*c*) 12·0 s; (*d*) 27·7 s; (*e*) 102 s.

in the same apparatus (figure 1), introducing an interior wall to produce a compartment 8·5 cm wide. Figure 8 is a shadowgraph showing the grid oscillating in the centre of this compartment for

$$\chi = \frac{2y}{w} = 0{\cdot}32, \tag{31}$$

a measure of the ratio of the width of the turbulent region (by (4)) to the compartment width w. Figure 8 (*a*) shows the regular, vertically periodic, structure that is shed from the grid in its initial motion. Some trace of the structure is seen near the grid at later times, but it appears to be quite local to the grid and not to persist throughout the turbulent region. After about 15 s, only 4·6 times the buoyancy period $2\pi N^{-1}$, layers of a larger scale develop near the boundary of the turbulent region (figure 8*d*). Since in this experiment the vertical group velocity of internal waves of horizontal length $\frac{1}{2}w$ and vertical length equal to twice the layer scale, 0·8 cm, is only 0·15 cm s^{-1}, it appears unlikely that the observed sequence of layers (for example, those shown in figure 8 (*d*), 27·7 s after the grid was started) could be produced by radiating waves within the time available. Dye showed motions away from the grid in the layers between the horizontal bands, which indicate regions of large density gradient in the shadowgraph. Groups of ten of these layers persist for period of 80 s or so, and the general pattern is retained for about 4 min before the layers break down into larger, less-coherent structures.

For larger values of the parameter χ, layers, although still visible in the still photographs (figure 9), become transient, lasting for only a few seconds, and for $\chi = 0{\cdot}64$ no layers are observed, the near-grid turbulent region filling a proportion $2\eta/w = 0{\cdot}60$ (using (4) and (31)) of the compartment.

As χ increases, the motions induced at a fixed distance from the grid will increase, and so the value of R at the sidewalls, the largest value of R in the compartment, will decrease. The absence of layers at large values of χ is thus in accord with the proposal that instability will occur only in regions of sufficiently large R, where R_f is expected to decrease with increasing R, such regions being excluded as χ increases. (A corollary is that in sufficiently long tanks conditions for instability will always occur.) The form of the layered structure and its development is similar to that found in numerical simulation of the instability by Posmentier, a regular array of alternating high- and low-density gradients being established in the initial stages, with the subsequent gradual evolution of larger layers.

The mean height of the regular layers seen in these experiments is shown by the crosses in figure 6 (*b*). They are a factor of about 1·5 times greater than the scale determined earlier by measuring the height of the intruding region of fine structure in the shadowgraphs, and this, as expected, is in good accord with the ratio 1·45 of average layer height to the scale h found in Ivey & Corcos' work (see §2). If we now equate the integral lengthscale of the turbulence at the edge of the turbulent region given by (17) with the height of the regular layers, rather than with the estimate of the scale h previously used, we find values of β (independent of the estimate of γ) equal to 0·35 for Ivey & Corcos' grid and 0·54 for our own. The latter is well beyond the range of values found by Hopfinger & Toly. It is thus plausible that the regular layer scale seen in figure 8 is *in excess of* the integral lengthscale of the turbulence (although proportional to it) and thus that the layers form on a scale *greater* than that of the turbulence itself, thus satisfying one of the conditions for the proposed stability analysis to be applicable.

It is interesting to note the similarity with observations of turbulent processes in rotating fluids. Whilst certain exact analogues exist between rotating and stratified

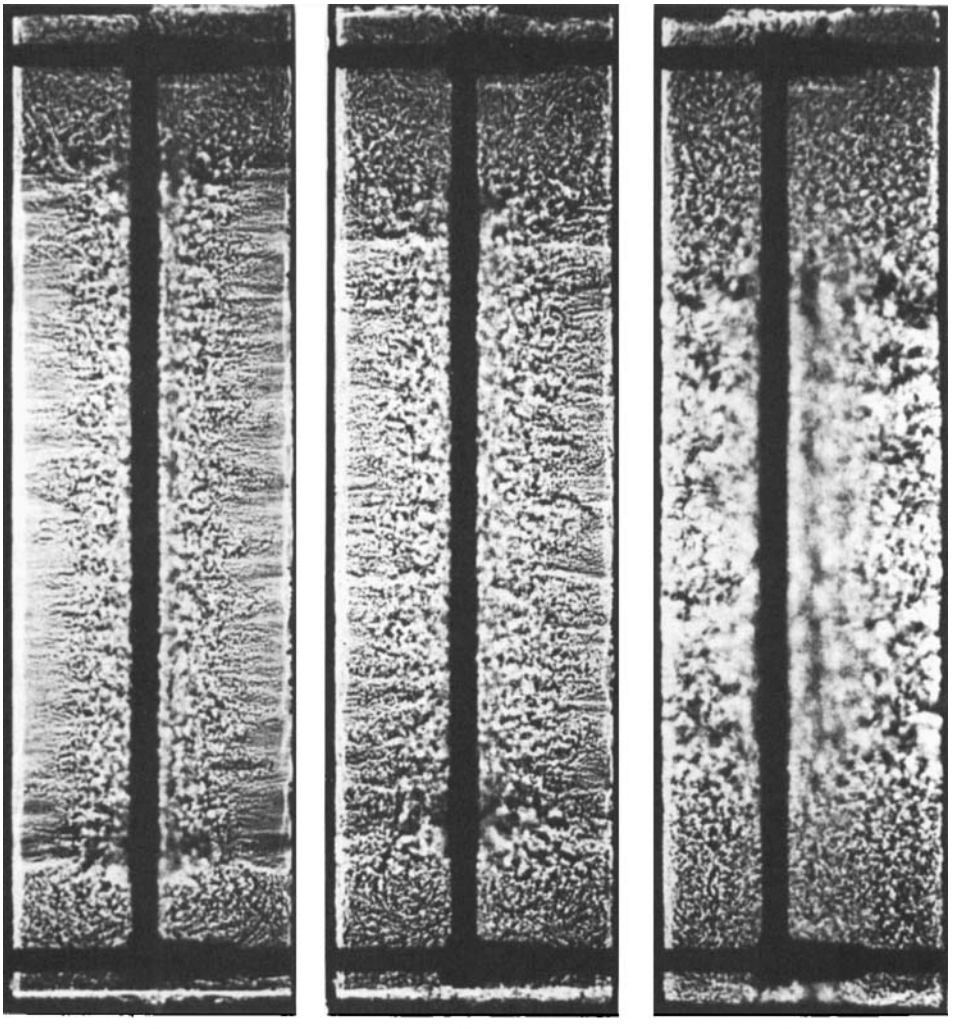

FIGURE 9. Shadowgraph experiments in a compartment 8·5 cm wide with grid oscillating in the centre. (*a*) $a = 0{\cdot}31$ cm, $\omega = 25{\cdot}7$ rad s^{-1}, $N = 2{\cdot}06$ rad s^{-1}, $\chi = 0{\cdot}40$, at time $t = 63{\cdot}5$ s after grid motion was started. (*b*) $a = 0{\cdot}31$ cm, $\omega = 34{\cdot}9$ rad s^{-1}, $N = 2{\cdot}02$ rad s^{-1}, $\chi = 0{\cdot}48$, at $t = 62{\cdot}5$ s. (*c*) $a = 0{\cdot}83$ cm, $\omega = 32{\cdot}6$ rad s^{-1}, $N = 1{\cdot}98$ rad s^{-1}, $\chi = 0{\cdot}64$, at $t = 62{\cdot}0$ s.

laminar flows, similarities in turbulent flows are poorly understood (but see Bradshaw 1969). McEwan (1976), following an idea proposed by Scorer (1966), showed experimentally that, in a tank of fixed height, *sufficiently weak stirring* at the horizontal boundary of a fluid in solid-body rotation about a vertical axis produced intense vortices. Following the laminar analogues, the corresponding condition in a stratified fluid would be that sufficiently weak mixing on a vertical wall of a tank of given width (that is at sufficiently small χ) would produce layers of large vertical density gradients. This is what has been observed. Whether there is a formal relationship between the two processes or coincidental similarity, and whether the turbulent stratified flow may, or may not, be unstable, have yet to be formally established. The experiments are suggestive but not conclusive.

The experiments were made whilst I was a visitor at the Research School of Earth Sciences at the Australian National University in Canberra. I am grateful for financial support by the R.S.E.S. and for the generous hospitality of Professor J. S. Turner, his encouragement, and many helpful comments during the course of the work. My thanks are also due to Mr Roy Potter (I.O.S.) who made the tank, to Messrs Derek Corrigan and Ross Wylde-Browne (R.S.E.S.) who helped to assemble and construct the apparatus and ably assisted with photography, and to Dr G. N. Ivey for sending details of his experimental results.

REFERENCES

AMEN, R. & MAXWORTHY, T. 1980 The gravitational collapse of a mixed region into a linearly stratified fluid. *J. Fluid Mech.* **96**, 65–80.

BRADSHAW, P. 1969 The analogy between streamline curvature and buoyancy in turbulent shear flow. *J. Fluid Mech.* **36**, 177–192.

DICKEY, T. D. & MELLOR, G. L. 1980 Decaying turbulence in neutral and stratified fluids. *J. Fluid Mech.* **99**, 13–32.

HOPFINGER, E. J. & TOLY, J.-A. 1976 Spatially decaying turbulence and its relation to mixing across density interfaces. *J. Fluid Mech.* **78**, 155–176.

IVEY, G. N. & CORCOS, G. M. 1982 Boundary mixing in a stratified fluid. *J. Fluid Mech.* **121**, 1–26.

KRANENBURG, C. 1982 Stability conditions for gradient-transport models of transient density-stratified shear flow. *Geophys. Astrophys. Fluid Dyn.* **19**, 93–104.

LINDEN, P. F. 1979 Mixing in stratified fluids. *Geophys. Astrophys. Fluid Dyn.* **13**, 3–23.

MCEWAN, A. D. 1976 Angular momentum diffusion and the initiation of cyclones. *Nature* **260**, 126–128.

MENDENHALL, C. E. & MASON, M. 1923 The stratified subsidence of fine particles. *Proc. Natn. Acad. Sci.* **9**, 199–202.

PHILLIPS, O. M. 1970 On flows induced by diffusion in a stably stratified fluid. *Deep-Sea Res.* **17**, 435–443.

PHILLIPS, O. M. 1972 Turbulence in a stratified fluid: is it stable? *Deep-Sea Res.* **19**, 79–81.

POSMENTIER, E. S. 1977 The generation of salinity fine structure by vertical diffusion. *J. Phys. Oceanogr.* **7**, 298–301.

SCORER, R. S. 1966 Origin of cyclones. *Sci. J.* **2**, 46–52.

THORPE, S. A., HUTT, P. K. & SOULSBY, R. 1969 The effect of horizontal gradients on thermohaline convection. *J. Fluid Mech.* **38**, 375–400.

TURNER, J. S. 1973 *Buoyancy Effects in Fluids.* Cambridge University Press.

WU, J. 1969 Mixed region collapse with internal wave generation in the density-stratified medium. *J. Fluid Mech.* **35**, 531–544.

WUNSCH, C. 1970 On oceanic boundary mixing. *Deep-Sea Res.* **17**, 293–301.